AD-A164 451 FLAW DETECTION OF PRESSURE VESSELS BY LASER-HOLOGRAPHIC 1/1
NON-DESTRUCTIVE D.. (U) FOREIGN TECHNOLOGY DIV
WRIGHT-PATTERSON AFB OH Z ZHENG 10 JAN 86
UNCLASSIFIED FTD-ID(RRS)T-1038-85 F/G 14/2 NL

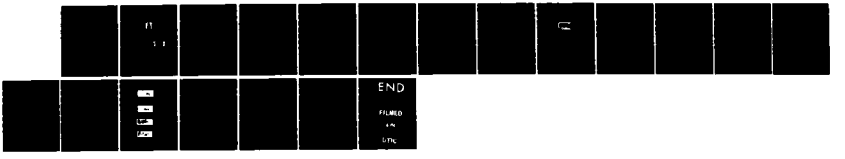

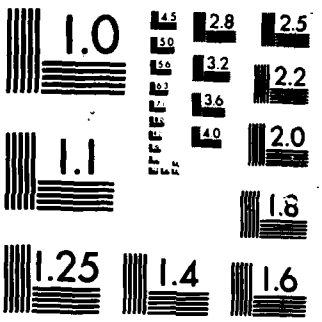

MICROCOPY RESOLUTION TEST CHART

NATIONAL BUREAU OF STANDARDS-1963-A

(2)

FTD-ID(RS)T-1038-85

AD-A164 451

FOREIGN TECHNOLOGY DIVISION

FLAW DETECTION OF PRESSURE VESSELS BY LASER-HOLOGRAPHIC NON-DESTRUCTIVE DETECTION (NDT) TECHNIQUE

by

Zheng Zhong-Zheng

DTIC
ELECTE
FEB 21 1986
S D
D

DTIC FILE COPY

Approved for public release;
distribution unlimited.

86 2 18 248

EDITED TRANSLATION

FTD-ID(RS)T-1038-85 10 Jan 86

MICROFICHE NR: FTD-86-C-001378

FLAW DETECTION OF PRESSURE VESSELS BY LASER-HOLOGRAPHIC NON-DESTRUCTIVE DETECTION (NDT) TECHNIQUE

By: Zheng Zhong-Zheng

English pages: 15

Source: Wusun Jiance, Vol. 6, Nr. 4, 1984, pp. 24-26

Country of origin: China
Translated by: SCITRAN
F33657-84-D-0165
Requester: FTD/TQTA
Approved for public release; distribution unlimited.

THIS TRANSLATION IS A RENDITION OF THE ORIGINAL FOREIGN TEXT WITHOUT ANY ANALYTICAL OR EDITORIAL COMMENT. STATEMENTS OR THEORIES ADVOCATED OR IMPLIED ARE THOSE OF THE SOURCE AND DO NOT NECESSARILY REFLECT THE POSITION OR OPINION OF THE FOREIGN TECHNOLOGY DIVISION.

PREPARED BY.

TRANSLATION DIVISION
FOREIGN TECHNOLOGY DIVISION
WP-AFB, OHIO.

GRAPHICS DISCLAIMER

All figures, graphics, tables, equations, etc. merged into this translation were extracted from the best quality copy available.

Accesion For	
NTIS CRA&I	☒
DTIC TAB	☐
Unannounced	☐
Justification	
By	
Dist ibution /	
Availability Codes	
Dist	Avail and / or Special
A-1	

Flaw Detection of Pressure Vessels by Laser-Holographic Non-Destructive Detection (NDT) Technique

Zheng Zhong-Zheng

Peking Institute of Chemical Engineering

The preliminary results of the laser-holographic non-destructive flaw detection tests of vessels with simulated flaws under hydraulic pressure are reported in this paper. The analysis and comparison of the deformative interference fringes of several types of flaw shapes and the rules of formation can be used as references for the judgement of the characteristics and sizes of flaws in the vessel under detection.

Large quantities of vessels with welded structure are used in the chemical industry. Since the 60's, the scale of production tends to be large; most vessels are made with high-strength, low-alloy stainless steels. Because the traditional methods of flaw detection have certain limitations, also because we hope to be able to attain quantitative detection results in order to calculate the safety criteria of the flaw sizes, based on the cracking mechanics, the laser-holographic flaw-detection method has some prominent advantages.

In this paper, we report the preliminary testing results, and the analysis and summary of the formation rules of the interference fringes of different flaw shapes. According to our testing results, we found that it is possible to attain useful quantitative information from the deformative fringes under some special conditions. The repetition of the results is also very good.

The Testing Arrangement, Testing Samples, and Testing Method

The testing uses the common double-exposured holographic arrangement. The light source is a 25 mw He-Ne laser. Due to the closed feature of the vessels, we used a hydraulic method to apply pressure to the vessels. The first exposure is made when the hydraulic pressure is attained at the scheduled value and the second exposure is made after the pressure has been released.

We used small vessels of 1Cr18Ni9Ti stainless steel with simulated flaws in the inner wall as testing samples. Each vessel has semi-cylinders A and B, and in each semi-cylinder different ring-like and axial grooves, with different depths and widths, were cut (Fig. 1. and Table 1.).

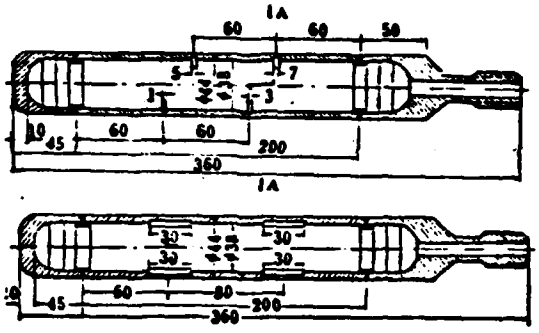

Fig. 1

Table 1. The Flaw Sizes of the Testing Vessels (mm)

No. of Vessel	Plane	Orientation of the Flaw	Width of Flaw		Depth of Flaw
			Left*	Right*	
#1	A	Ring-direction	5	7	0 ~ .15
	B		3	1	
#2	A	Ring-direction	5	7	0 ~ 1
	B		1	3	
#3	A	Axial-direction	5	7	1
	B		1	3	
#4	A	Axial-direction	7	5	.8
	B		1	3	

* The left and right sides are defined with the front view in which the water tube is on the right .

During the testing, one of the end of the sample vessel was clamped horizontally in a vibration-isolated platform, and the other end (sealing end) was connected with the testing pressure pump by a flexible water tube to apply hydraulic pressure.

In order to attain a good basis for comparison of all the holographic pictures it is necessary to use the same optical path arrangement. Therefore we arranged the illumination and observing directions as fixed in the horizontal planes of the axial line of the vessels, and made them overlapping with the normal direction of the axis or intersecting it with a small angle to compensate the axial movement due to the clamping and water tube, thus making the double-exposured holographic pictures of the flaw-free vessels have uniform, symmetric flat-oval fringes of interference. (Fig.2*).

Attention should be paid that there should be no any tiny displacement of the rigid body during the exposure process. For example, un-tightened clamping of the vessel, too fast unloading or loading of the pressure, etc. will cause an increase of the fringe number and change of the fringe shapes.

* It is mistaken as Fig. 1 in the original Chinese paper.

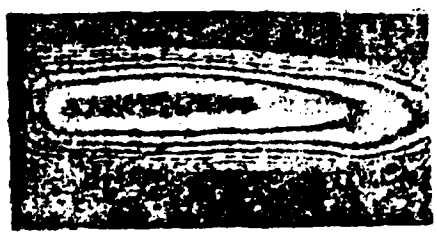

Fig. 2

Fig. 2. Double exposure hologram of flawless pressure vessel $\Delta P = 100 kg/cm^2$.

Although this does not influence the qualitative judgement of the position and area of the flaws, it has influence if we try to quantitatively judge the shapes of the flaws, orientations and sizes of the flaws. Fig.3 is a sketch of the arrangement of the light route. The ratio of light intensities, and the exposure parameters are all within the normal range.

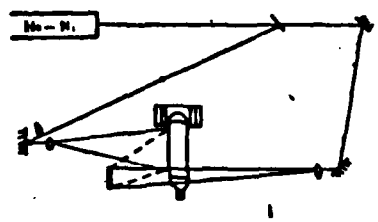

Fig. 3

Fig. 3. Light route arrangement diagram.

The Analysis of the Testing Results

The testing is done under different pressure loadings (10 - 200 kg/cm^2 with step 10 kg/cm^2). The double-exposured holographic pictures were made for the two semi-cylinders from the outside for each testing vessel, and each picture includes the interference fringes of the left and right-side flaws. We attained 8 groups of holographic pictures altogether. We also obtained the double-exposured holographic' pictures of a flaw-free, inner pressured vessel to offer the basis of comparison.

1.The analysis of the holographic pattern of flaw-free, inner-pressured vessels.

For the thin-wall-cylinder vessels (that is: the ratio of the outside diameter to the inner diameter $\leq$ 1.2 or the ratio of wall thickness to the inner diameter $\leq$ 1/10), according to the zero-torque theory, we know that when the inner wall undergoes a uniform inner-pressure in the vessel body at the middle of the cylinder, the diametrical expansion and axial stretch will be generated as per the following formulas:

The diametrical displacement is: $W = (2 - \mu) \frac{Pr^2}{2ES}$

The axial displacement is: $U = (1 - 2\mu) \frac{Pr}{2ES} \cdot x$

The stresses at the cylinder body are as follows:

The ring-direction stress: $\sigma_1 = \frac{Pr}{S}$

The axial direction stress: $\sigma_2 = \frac{Pr}{2S}$

Here: P is the pressure, r is the diameter of the cylinder, S is the thickness of the cylinder wall, E is the modulus of elasticity of the material, μ is the Poisson coefficient of the material (usually equals to 0.3), and x is the axial coordinate of the vessel.

We can know from the these formulas that the axial displacement changes with X. At the position of X = r, the axial displacement is a quarter of the diametrical displacement, and the ring-direction stress in the cylinder wall is twice the axial stress.

According to the principle of interference, we know that the orientation of the fringes is perpendicular to direction of the deformation. Therefore, the horizontal fringes in Fig.2 show the diametrical expansion of the vessel, and the vertical fringes show the deformation in the axial direction. Because the interference fringes are the trace with the same optical-path difference, therefore the fringes usually show the the total displacement and will show the single-direction displacement only in some special conditions. But it is yet possible that the

presented single-direction displacement also could be the result of multi-directional displacement. Therefore, combining the physical meaning, it needs further analysis and distinguishing.

Usually, if we want to calculate the value of displacement at some position of the body, we should know the orders of the fringes. But for the diametrical expansion and the axial stretch of the flaw-free pressure vessel, there is no fixed point. There is no zero order fringe. But because the direction of diametrical displacement is known and is the major displacement, we can use the above optical arrangement to obtain holographic patterns of the vessels. (Figure 2) And the group of the horizontal fringes of the middle part of the vessel, except the both ends which are influenced by the boundaries, is a manifestation of the uniform diametrical expansion of the vessel; each fringe is related to the diametrical displacement under some load. But because of the viewing-difference in the plane view only the fringes in the axis are truly related to the real value of the axial displacement. The diametrical displacement related by the horizontal fringes which are outside of the vessel axis varies with cosine of the central angle of the fringe. Under a certain load, the diametrical displacement of the vessel can be calculated with the above formulas. Therefore,

the fringes of the holographic pattern at the axis, under the same load, are correlated to the values of such displacement. When the deformative fringes are due to the existence of the flaws, the deformative fringes have the same characteristics as described above. New fringes will be generated in the positions with big deformation, making the number of fringes (and orders) increase. Because the displacement difference of each order of fringe is equal to the half wavelength of the laser light, the absolute displacement can be known by calculating the related position of the deformative fringes and the increase of the order at the point concerned. This basic understanding can be used as a base to analyse the deformative fringes described below:

2. The analysis of the holograghic patterns of the ring-direction grooves

Fig. 4 is the A-plane double-exposured holographic pattern of vessel #1, with a load of 60 kg/cm^2. From the fringe we can see the originally very flat oval fringes at the middle part of the vessel have un-continuous deformative fringes at positions of the ring-direction grooves at both vessel sides. 'Closed' oval deformative fringes appear at the centers of the grooves and at their left and right-sides. At the upper and lower ends of the grooves, V-shape valleys with different width appear in

the picture. The width of the opening of the V-shape is same as the measured width of the groove. The outmost part of the V-shape fringes is a manifestation of the length of the groove. The centerward fringes mean that the order of the fringes is increasing, a result of the increased deformation. And the increase of the order of the deformative fringes is a result of the increase of the load. But the order of the deformative fringes of the wide groove at the right side is 1-2 orders higher than that of the left side, showing the difference caused by the wide groove and the large deformation. The upright shape and the symmetric curvatures of the new-generated deformative fringes mean that the axial deformation is the major one. This is consistent with the actual situation that the left side and right side of the vessel, at the ring-direction grooves and under inner pressure, will generate additional axial displacement with opposite directions. The distribution of vertical fringes is a record of the regions which will undergo deformation when the grooves are under pressure.

Fig. 5 is the B-plane holographic pattern of the vessel #1. The load is also 60 kg/cm^2. We can see from the figure that at the centers of the grooves no closed oval fringes are formed, but the V-shape fringes become more vertical and sharp. We can judge the width and length of

the groove from the size of the opening and the shape of the valley of the V-like fringe. The left side has a one order increase compared with the right side. The deformative fringes at the inside of the two grooves in Fig. 5 have one a oneorder :rease compared with the outside ones. This situation can be explained by the stress concentration at the narrow groove. The vertical fringes at the left groove in fig. 5 are very dense. This means the gradient of the axial strain is large and the one-order less for the outside fringes is due to the influence of the boundary conditions at the two ends.

The comparison of the above holographic patterns uncovers the different characteristics of the deformation fringes of grooves with different widths.

Fig. 4. A-Plane of Vessel #1, Δp=60 kg/cm^2

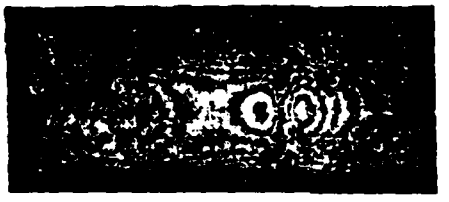

Fig. 5. B-Plane of Vessel #1, Δp=60 kg/cm^2

Fig. 6. A-Plane of Vessel #3, Δp=40 kg/cm^2

Fig. 7. B-plane of Vessel #3, Δp=40 kg/cm^2

3. The analysis of the holographic patterns of the axial grooves.

Fig. 6 and 7 are the A and B-plane holographic patterns of vessel #3. The loads are all 40 kg/cm^2. We can see from the Figures that the correspondence of the deformative fringes and the actual positions of the grooves are very good, and all are closed ovals. The increase of the fringe orders is very fast. This truly reflects the characteristics of the axial grooves which are easily deformed and will produce ring-direction displacement deformation. Under very small load ($10kg/cm^2$), the deformative fringes are very clear. When the load increases the upper and lower sides also appear as closed fringes and this gives out the true characteristics of the longitudinal expansion of the axial grooves. Under large load, the number of closed ovals increase. The long axis of the outermost oval usually exceeds the actual length of the groove; this is the result of the correlated deformation. But the distance between the oval fringes formed by correlated deformation will certainly be widened. Therefore, only taking the long axis of the oval with uniform fringe distance at the both ends, we can decide the length of the flaw accurately.

Preliminary Results

Laser holography as a technique of non-destructive detection is able to be applied to the flaw detection of thin-wall vessels. The results show the distribution of displacement of the whole field. It can be used not only to show reliably the positions of the flaws by the deformative fringes of interference, but also can be used to decide the orientation planes and the sizes of the flaws. The total deformative displacements at the flaws can also be estimated by the analysis of the fringes of the whole field to attain semi-quantitative results. This technique can also be used to show the characteristics of the deformation and the region of the influence. Therefore it can be considered for the application to the structural analysis of vessels, such as the studies of the regional load and concentration of the stress, etc. But the results of this paper are based on artificially simulated flaws. This is of course much more simple than the complicated real flaws. But the already attained results and experience will certainly be valuable for practical applications.

References

[1] Charles M. Vest, "Holographic Interferometry" John Wiley & Sons, New York, N. Y., 1979.

[2] Metals Handbook, Vol.11, "Nondestructive Inspection and Quality Control" 8 ed., American Society for Metals, 1976.

[3] Erf, R. K. (ed.), "Holographic Nondestructive Testing" Academic Press. London & New York, 1974.

[4] Harry, J. Saxton, et al., "Behavior of Flawed Pressure Vessels" 3rd International Conference on Pressure Vessels Technology, Part 1, pp.489-505.

[5] "Flaw Detection in Thin Composite Material Structure with Holographic Techniques." AD-AO 21942, 1976.

FLAW DETECTION OF PRESSURE VESSELS BY LASER HOLOGRAPHIC NDT TECHNIQUE

Zheng Zhongzheng

(Beijing Institute of Chemical Technology)

Four simulative flawed pressure vessels are subjected to hydraulic pressure for the detection by laser holographic method. The characteristic of the fringe patterns due to the deformation of the flaws provides some valuable information which can be applied to evaluate the behavior and size of practical flaws in pressure vessels.

END

FILMED

3-86

DTIC